Polyurethane scaffold formation via a combination of salt leaching and thermally induced phase separation

Heijkants, R. G. J. C.; van Calck, R. V.; van Tienen, T. G.; de Groot, J. H.; Pennings, A. J.; Buma, P.; Veth, R. P. H.; Schouten, A. J.

Published in:
Journal of Biomedical Materials Research. Part A

DOI:
10.1002/jbm.a.31829

Publication date:
2008

Polyurethane scaffold formation via a combination of salt leaching and thermally induced phase separation

R. G. J. C. Heijkants,[1] R. V. van Calck,[1] T. G. van Tienen,[2] J. H. de Groot,[1] A. J. Pennings,[1] P. Buma,[2] R. P. H. Veth,[2] A. J. Schouten[1]

[1]*Department of Polymer Chemistry, Faculty of Mathematics and Natural Sciences, University Groningen, Nijenborgh 4, 9747AG Groningen, The Netherlands*

[2]*Orthopaedic Research Laboratory, University Medical Center, P.O. Box 9101, 6500HB Nijmegen, The Netherlands*

Received 8 May 2006; revised 26 April 2007; accepted 20 July 2007
Published online 28 January 2008 in Wiley InterScience (www.interscience.wiley.com). DOI: 10.1002/jbm.a.31829

Abstract: Porous scaffolds have been made from two polyurethanes based on thermally induced phase separation of polymer dissolved in a DMSO/water mixture in combination with salt leaching. It is possible to obtain very porous foams with a very high interconnectivity. A major advantage of this method is that variables like porosity, pore size, and interconnectivity can be independently adjusted with the absence of toxic materials in the production process. The obtained compression moduli were between 200 kPa and 1 MPa with a variation in porosity between 76 and 84%. Currently the biological and medical aspects are under evaluation. © 2008 Wiley Periodicals, Inc. J Biomed Mater Res 87A: 921–932, 2008

Key words: polyurethane; scaffold; meniscus; degradable; thermally induced phase separation

INTRODUCTION

In vivo tissue engineering of different damaged or removed tissues nowadays attracts a lot of attention in biomedical research. The search for suitable polymeric systems includes the search for polymers with a tunable degradation rate in combination with preparation methods for optimal scaffolds.

A great variety of methods and materials have been reported in literature. Techniques mentioned include particulate leaching,[1–3] gas blowing,[4] freeze-drying,[5] 3D-printing,[6] thermally induced phase separation (TIPS),[7–10] electrospinning,[11] and particle sintering,[12] or combinations of these. All of these methods are meant to yield porous scaffolds with interconnected pores to allow tissue ingrowth. High porosity is generally recommended to reduce the amount of implanted material and to create a large surface on which cells can adhere.

It is also known from literature that the cell size around 150–350 μm of the foam is of great importance for the correct cell ingrowth.[13–16] Moreover, interconnectivity, the connection between the pores in the scaffold, is very important since it plays a decisive role in the diffusion of cells into the scaffold and the transport of nutrients and cellular waste products.[16–20] The minimum interconnecting openings should be at least 10–12 μm. An accurate control over the interconnectivity independent of the pore size and overall porosity is therefore necessary. For polyesterurethanes, however, this is a factor that cannot be controlled well by the methods mentioned in literature. Guan et al.[10] used semi-dilute DMSO solutions of a polyesterurethaneurea where upon cooling down to −20 or −80°C the solvent crystallized, and after washing at −20°C a highly porous scaffold was obtained. The structures presented reveal, however, a poor interconnectivity, which is also suggested by the long washing times needed to remove the solvent. Gorna and Gogolewski[21] showed a technique based on a polyurethane solution in a good solvent to which a nonsolvent was added to obtain phase separation. This mixture was solidified and subsequently the (non)solvent mixture was removed using water. De Groot et al.[22,23] and Van Tienen et al.[24] presented highly porous foams prepared by salt leaching phase separation and solvent crystallization from a polyesterurethane. However, the resulting foams exhibited macropores originating from the salt crystals with interconnecting micropores originating from solvent crystallization. Their conclusion was that these structures were unsuitable for implantation. Apart from the above-described cell size, porosity, and intercon-

Correspondence to: A. J. Schouten; e-mail: a.j.schouten@rug.nl

nectivity, suitable mechanical properties are also required in many applications.

In the forgoing studies of our group we focused on the *in vivo* tissue engineering of meniscus tissue, either by repairing a damaged meniscus by introducing a plug[25] or by complete reconstruction of the meniscus.[22] So far, the choice of the polymers as well as the choice of the scaffold appeared to be not optimal.

In this study, the production of polymeric scaffolds that meet the above-described requirements is presented. This new method is based on a combination of thermally induced phase separation and/or crystallization and salt leaching using poly(ε-caprolactone) (PCL)/1,4-butanediol/1,4-butanediisocyanate-based polyesterurethanes described previously.[26] The different factors that influence the scaffold structure and the mechanical properties of the scaffold are described. In addition the use of potentially toxic solvents is circumvented. The foams prepared were implanted subcutaneously in rats[27] and in the knees of dogs and the results have been evaluated until 6 months of implantation. The ingrowth was already complete at 6 months of implantation. Type II collagen was observed. This biological evaluation has been published elsewhere.[28]

EXPERIMENTAL PROCEDURES

Materials and methods

Dimethylsulfoxide (DMSO, Acros) was distilled under reduced pressure from CaH_2. Sodium chloride crystals (Merck) were sieved to the mentioned size using NEN standard test sieves from Wilten (Etten-Leur, The Netherlands). Ethanol, ether, and hexane (Lab-Scan, Dublin, Ireland) were used as received.

The polyurethanes used here are based on a soft segment of PCL prepared by thermal ring-opening polymerization of ε-caprolactone, initiated with 1,4-butanediol, leading to polymers with different molar masses (1000, 1600, 2200, and 2800 g/mol). The hard segment is based on 1,4-butanediisocyanate and 1,4-butanediol and has a uniform length. The synthesis is described elsewhere.[27] In short, the polyester precursor was prepared in bulk at 150°C for 7 days. The prepolymer was endcapped with six-fold excess of BDI at 80°C under argon atmosphere. The reaction time was 4 h. The excess BDI was removed by short-path distillation. The end-capped polymer was chain extended with BDO in bulk at 80°C for 16 h under argon atmosphere. PU*x* indicates the polyurethanes with *x* as the molar mass of the PCL segment. The complete polymerization was carried out without the use of catalyst and solvent to ensure a minimum of side reactions, and to prevent the use of any possible toxic products.

An Ubbelohde viscometer (type Oa) was used for the determination of the intrinsic viscosities in chloroform at 25°C. Molar masses (M_n and M_w) and molar mass distribution (M_w/M_n) of the polyurethanes were determined by GPC measurements using dimethylformamide with 0.01*M* LiBr as eluents on a Waters 600 Powerline system, equipped with 2 mixed-C Plgel 5μ columns (Polymer Laboratories) kept at 70°C. The data-analysis was done using conventional calibration with polystyrene standards.

A TA-Instruments modulated DSC (DSC 2920) was used for studying thermal transitions. When mentioned a TA-Instruments DSC, Q1000 was used instead. The heating and cooling rates were 10°C/min, unless mentioned otherwise.

A Jeol 6320 F field emission scanning electron microscope (FESEM) was used for studying the pore structure of the porous materials. It was operated at a working distance of 11 mm, an acceleration voltage of 5 kV, and a beam current of 1×10^{-10} A. The specimens were made conductive with a 3-nm layer of gold using a Cressington rotating magnetron sputter coater operated at a working distance of 150 mm and a current of 20 mA. All the pictures were taken from inner surfaces obtained by cutting the sample with a sharp razor blade, unless mentioned otherwise.

Compression tests were performed on cubic-shaped specimens of about 5 mm × 5 mm × 5 mm cut manually from the scaffolds. The experiments were performed at 21°C with a 100-N load cell and a strain/compression rate of 2 mm/min using an Instron (4301) mechanical tester. The compression modulus was determined at 20% compression. Each sample was measured in each direction and the values were averaged. Infrared spectroscopy (ATR-FTIR) was done using a Bruker IFS88 equipped with a Golden Gate (Graseby Specac) ATR accessory equipped with a Heated Top Plate Mk 2. Foam samples of about 2 mm × 2 mm × 2 mm were placed on the diamond element and compressed at room temperature with 40 cNm. FTIR spectra at different temperatures were obtained by taking 100 scans at a resolution of 2 cm^{-1}. Spectra were compared after scaling of the maximum of the ester carbonyl peak.

DMSO remains were determined via sulfur detection using an Euro EA elemental analyzer of Euro Vector instruments. NaCl remains were determined using a Perkin & Elmer 1100B atomic absorption spectrometer (AAS).

Foam preparation

The PU*x* polymer was dissolved in DMSO (35 wt % solution) at 80°C, after which between 0 and 11% R.O. water (based on the total amount of solvent) was added to decrease the quality of the solvent for the polymer. Sodium chloride crystals (preheated to 130°C), sieved to a particle size of 150–350μm, were added to the solution at 80°C. The mixture was transferred to a Teflon mould (as shown earlier[29]) or a round glass mould of 4 cm in diameter and 2 cm high, and cooled either to room temperature or to −18°C. The NaCl and solvent were removed by washing at room temperature with excess of R.O. water containing 20% ethanol. One liter of solution was used per gram of polymer. The solution was renewed after 12 h. After washing with the water/ethanol mixture for 20 h, the foam was washed for 1 h with 0.2 L 96% ethanol per gram of polymer to remove the last traces of the solvent. In some cases the foam was also washed with ether or hexane. Finally, the foam was dried under vacuum at 37°C for 24 h.

Determination of the porosity of the foam

The porosity of the foams was determined by measuring the dimensions and the mass of the foam and calculated as follows:

$$p = 1 - \frac{m}{\rho_{polymer} \cdot V}$$

where p is the porosity, m is the mass of the scaffold, $\rho_{polymer}$ is the density of the polymer, and V is the volume of the scaffold.

RESULTS AND DISCUSSION

Foam preparation

The polymer concentration is a very important factor in foam preparation. In principle this should be as high as possible, but the homogeneous admixing of nonsolvent and NaCl should still be possible. In practice, the compromise was 35% (w/w). As described previously, the chain extension of the PU*x*'s was performed in the bulk and not all reactive groups disappeared.[27] When these polymers with varying hard-segment content were dissolved for foam formation the molar mass increased further (Table I). By varying the time that the polymer is in solution, the molar mass of the final foam can be maximized with respect to solubility and mixability of the porogen. In this manner, the nonsolvent can be added at the moment where the solution is still just stirrable. During washing the last few remaining isocyanate groups will be removed by reacting with water.

When a polymer is dissolved in a poor solvent at elevated temperatures, phase separation takes place upon cooling the solution. A polymer-rich phase and a polymer-lean phase are formed according to the phase diagram of the polymer in that solvent.[30] When this process is carried out with concentrated solutions, phase separation can be stopped before two completely separated layers are formed, thereby creating the basis of a foam structure. Moreover, when the polymer solution is mixed with insoluble particles, which can be washed out in a later stage with a nonsolvent for the polymer, porosity and pore structure can be tuned. In our case, DMSO and water were used as solvent and nonsolvent, which are both also considered not to be toxic in minor concentrations. DMSO is used in the medical field as a radical scavenger and generally accepted as biocompatible.[31,32] The use of nontoxic components during the production will prevent the presence of toxic materials in the end product.

Preheated, sieved NaCl crystals of a certain size were mixed into this solution at 80°C. It is assumed that NaCl is insoluble in the polymer solution and that it has no significant influence on the phase separation system, even though it is known that it can have some influence on the phase behavior of the DMSO/water mixture.[33]

TABLE I
Molar Mass After Foam Formation

	$[\eta]_{before}$ (dL/g)	$[\eta]_{after}$ (dL/g)	M_n (kg/mol)	M_w (kg/mol)	PD
PU1000	0.39	0.89	69.8	161.8	2.3
PU1600	0.56	1.33	86.2	273.8	3.2
PU2200	0.57	1.08	80.5	177.1	2.2
PU2800	n.d.	n.d.	99.4	295.7	3.0

n.d., not determined.

The polyurethanes used in our study are composed of two segments, which are both able to crystallize in principle whereas two different phase separation processes may take place.[26]

The following processes are considered:

1. Crystallization of the hard segments before or after liquid–liquid phase separation.
2. Crystallization of the soft segments before or after liquid–liquid phase separation.
3. Macrophase separation because of total polymer insolubility.
4. Microphase separation between hard and soft segments in the polymer chain.

The influence of two different cooling procedures was investigated: cooling to room temperature and cooling to −10°C.

Cooling to room temperature

In this case, two transitions can occur. Depending on the amount of water that is used as nonsolvent, liquid–liquid phase separation can occur. The polymer solution separates into a polymer-rich phase and a polymer-poor phase. As one would expect, the addition of nonsolvent will decrease the solvent quality, and hereby increase the temperature at which L–L phase separation occurs. This influence of the amount of nonsolvent on the L–L phase separation temperature has been confirmed visually and with DSC.[34] For a 35 wt % solution of PU1600 polymer in DMSO without water no L–L phase separation was found, while with a water content of 6.75% a polymer-rich and lean phase appeared just below 75°C. Clearly an increase in water concentration leads to a major increase in L–L phase separation temperature.

Moreover, it was found that the mixture gels upon cooling or during annealing at 20°C. Modulated DSC was used to determine the cause of this gelation.

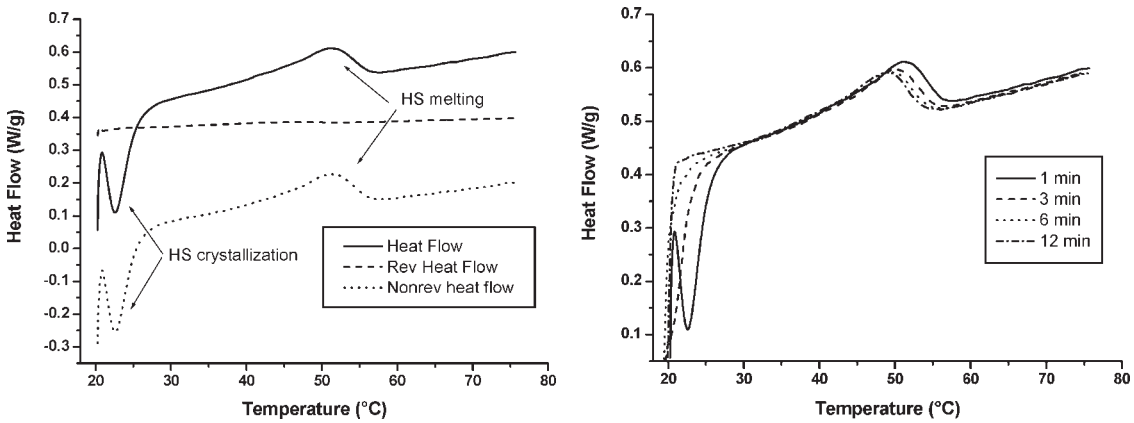

Figure 1. Heating curves of PU1600 (35% w/w) solution in DMSO containing 4.1% water. Left graph shows a modulated DSC scan with 1°C/min from 20 to 80°C after cooling from 80 to 20°C with the same speed. The right graph shows up-scans from 20 to 80°C after different annealing periods at 20°C.

PU1600 was dissolved in DMSO (35% w/w) with 4.1 wt % of water as nonsolvent. This mixture was kept at 80°C for 5 min after which it was cooled with 10°C/min to 20°C and kept at this temperature for 1 min (with 3.4% water it was found that the system phase separates at about 45°C.) Subsequently, the sample was heated to 80°C with 1°C/min and a modulation of 0.5°C per 60 s. The left thermogram of Figure 1 shows the result. It is clearly visible that in the nonreversible heat flow, an exotherm is found at 23°C and an endothermic peak around 50°C is present. This can be interpreted as crystallization and melting of the hard segment, since the soft segment is better soluble in DMSO than the hard segment. There is also a clear difference between the scans with different annealing times at room temperature. The right picture of Figure 1 shows up-scans after 1, 3, 6, and 12 min of annealing at room temperature. The exothermic peak disappears completely with increasing annealing times, whereas the melting peak at 55°C remains constant. Apparently, an annealing time of 1 min was not long enough to complete the crystallization at 20°C. The maximum melting peak shows a slight decrease in temperature with increasing annealing time. This also supports the above-mentioned explanation of crystallization of the hard segment, since it is generally known that an increase in crystallization temperature causes an increase in melting point.

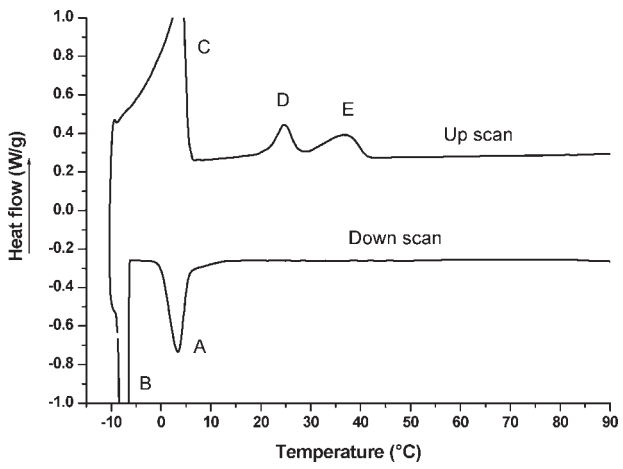

Figure 2. Cooling and subsequent heating modulated DSC traces for a 35% PU1600 solution in DMSO containing 5.7% water. Before the up-scan the sample was kept at −10°C for 5 min. A: Crystallization of hard segment. B: Crystallization of DMSO. C: Melting of DMSO. D: Melting of PCL that crystallized at B. E: Melting of hard segment that crystallized at A.

Cooling to −10°C

On cooling further to −10°C or lower, freezing of DMSO can be expected, in addition to the above-mentioned phenomena. A difference with cooling to room temperature is that the sample is not annealed at 20°C which means that the hard segment will

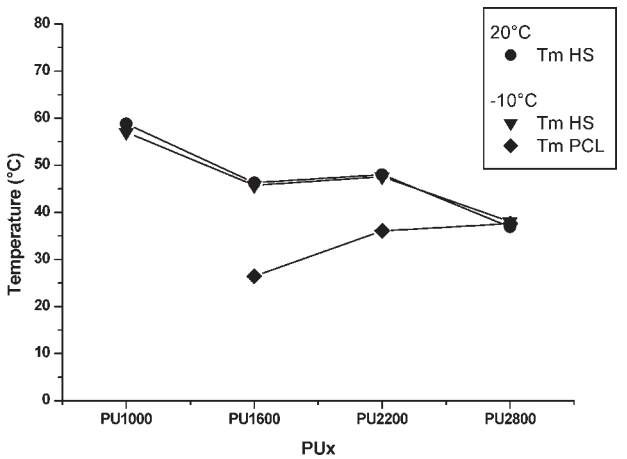

Figure 3. Melting points of 35% PU1000, 1600, 2200, and 2800 solutions in DMSO containing 5.7% water after cooling to 20°C and −10°C.

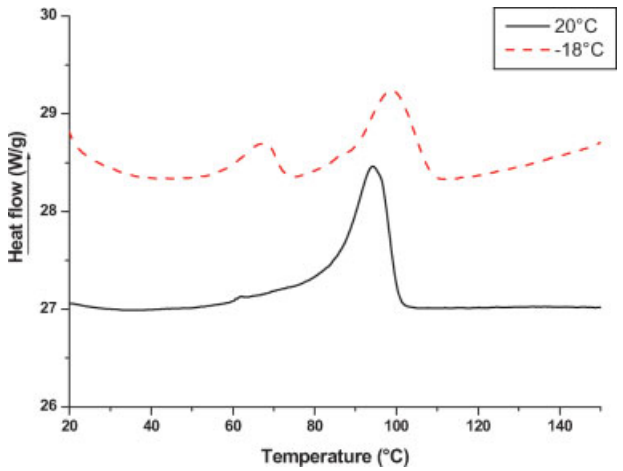

Figure 4. Melting behavior difference of two foams prepared from PU1600 by cooling down a NaCl suspension in a 35% (w/w) solution in DMSO to −18°C or by annealing at 20°C for 1 h (DSC Q1000). [Color figure can be viewed in the online issue, which is available at www.interscience.wiley.com.]

crystallize during cooling anywhere between 20°C and the temperature at which DMSO crystallizes.[30] To elucidate this, a 35% PU1600 solution containing 5.7% water was cooled to −10°C in the DSC (Fig. 2, lower curve). In this case DMSO freezes at about −8°C (peak B), and crystallization of hard segment can be observed at +8°C (peak A). The up-scan in Figure 2 shows two melting peaks. The peak at 36.8°C (peak E) is because of melting of hard segment that crystallized before the freezing of solvent. Peak D, however, is ascribed to crystalline PCL, supported by the fact that this peak is not present when the hard-segment content of the polymer increases, while a decrease in hard-segment content leads to a higher melting point (Fig. 3). Apparently, the PCL is able to crystallize as soon as the undercooling increases or because of the increased polymer concentration as a result of DMSO crystallization.

As can be seen in Figure 4, the double melting peaks can also be found in the final foams (after washing as will be explained later), although both are found at higher temperatures because of the absence of solvent. The high-temperature peak originates from hard segment that crystallized before the solvent froze. The low-temperature melting point has to be ascribed to crystalline PCL produced during the cooling period below room temperature. This peak has a melting enthalpy of 5.5 J/g, which corresponds to 3.3% crystalline PCL.[36] The foam cooled to room temperature shows one peak at 94.2°C. This originates from crystallized hard segment without the freezing of solvent.

Although in principle microphase separation could interfere in several steps of the procedure, no indication of this was found at any step. At least no indication of amorphous hard-segment phases was found and therefore it is concluded that this process, if it occurs at all, is followed directly and completely by hard-segment crystallization.

The origin of the double melting peak in solution and of the foams was further confirmed by ATR-FTIR measurements at different temperatures of foams made by either cooling to −18°C or to room temperature (Fig. 5). The spectra show the carbonyl absorptions of the ester groups of PCL (1726 cm^{-1}), the amide I (1681 cm^{-1}), and the amide II (1535 cm^{-1}) of the urethane group. The difference between the absorptions in the melt and in the crystalline state are clearly observed comparing the spectrum at 120°C with the spectra at lower temperatures. The Amide I has disappeared completely from that position and has moved toward the PCL ester absorption. Moreover, it is seen from Figure 5 (right figure) that heating to a temperature above the first melting peak (60°C) in Figure 4 does not lead to any change in the spectrum. This is clearly evidence that the first melting peak is not related to the melting of hard-segment crystals. If the additional melting peak orig-

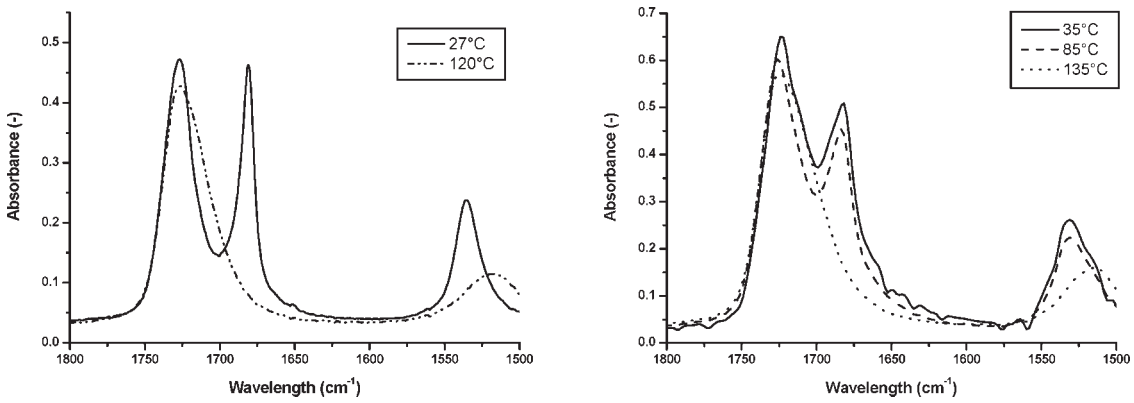

Figure 5. ATR-FTIR spectra taken of PU1600 foam. Left: cooled to room temperature, which does not contain crystalline PCL. Right: cooled to −18°C, which does contain crystalline PCL.

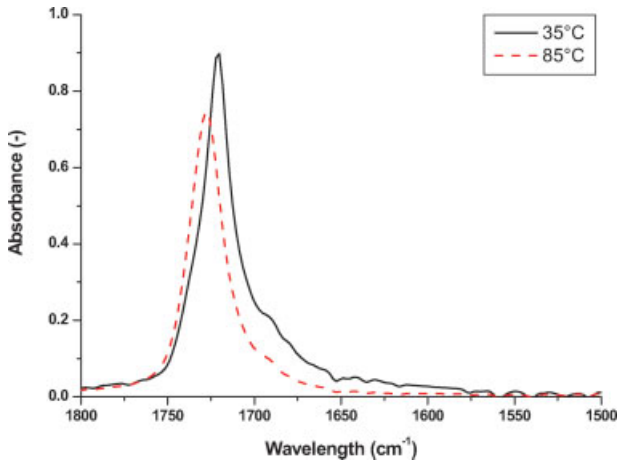

Figure 6. ATR-FTIR spectra of PCL taken at 35 and 85°C. [Color figure can be viewed in the online issue, which is available at www.interscience.wiley.com.]

inates from crystalline PCL a small shift is expected (Fig. 6), but since the melting peak had a melting enthalpy of only 5.5 J/g, which corresponds to a crystallinity of 3.3%, the change in the ester peak absorption is not observable at all.[36]

Washing

After cooling, the suspension was washed with a nonsolvent for the polymer. In this case water containing 20% of ethanol is used. NaCl, DMSO, and water were removed after extensive washing, leaving a foam.

As a last step the foam was washed with 96% ethanol. This step ensures the removal of the last traces of DMSO. The complete removal of DMSO and NaCl was confirmed with AAS. In the case of the PU1600 foam it was found that less than 0.11 wt % of NaCl was present in the foam, while elemental analysis showed that the amount of sulfur present in the foam was below the detection limit of 0.01 wt %, indicating that no significant amount of DMSO was present anymore. Moreover, the obtained foams showed hardly any shrinkage after drying. From this it can be concluded that the initial polymer concentration determines the overall porosity, and that the foam structure had a very high interconnectivity with opening diameters larger than 10–12 μm which are large enough for blood vessel ingrowth.

In some cases the foam was subsequently washed with ether to remove the skin (see later). With the above-described method an open porous polymeric foam was obtained.

Foam properties

Influence of phase diagram trajectory on foam structure of PU1600

Foam formation without addition of water

Figure 7 presents the SEM pictures of two different foams, prepared by cooling down to −18°C and by cooling to room temperature of polymer solutions without addition of water. Clear differences can be seen in the microstructure of the cell walls. As was shown before, no L–L phase separation occurs during cooling in this case. The left picture also shows no indication of this. Only a small amount of imprints of solvent crystals around the holes formed by the NaCl can be found, which shows that in this case the structure is mainly formed by the NaCl crystals.

Cooling to room temperature only gives the foam a different cell wall structure, as can be seen in the right picture. In this case the hard segments apparently had more time to crystallize and formed big spherulitic structures, seen as spheres. Although it was possible to remove the solvent and NaCl from these foams, there is hardly any interconnectivity between larger pores. The difficult removal of the NaCl and DMSO in the preparation procedure can correspond with this observation.

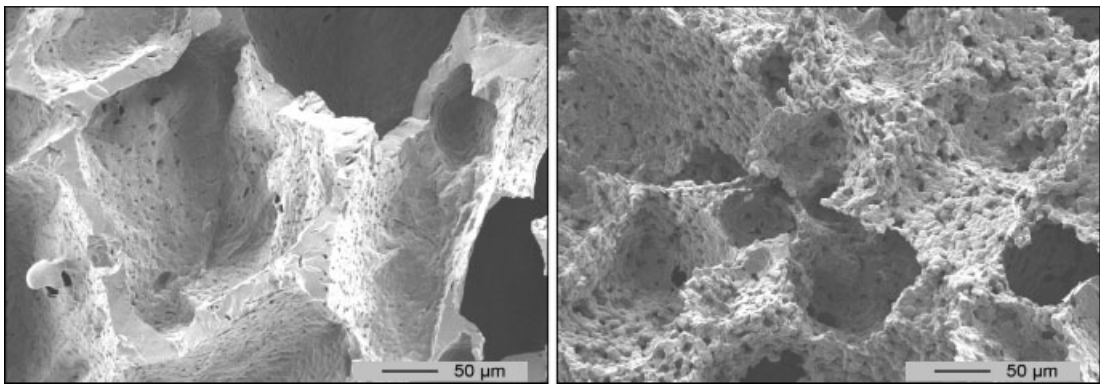

Figure 7. 35% PU1600 in DMSO without water. Left: frozen at −18°C before washing. Right: cooled to room temperature before washing.

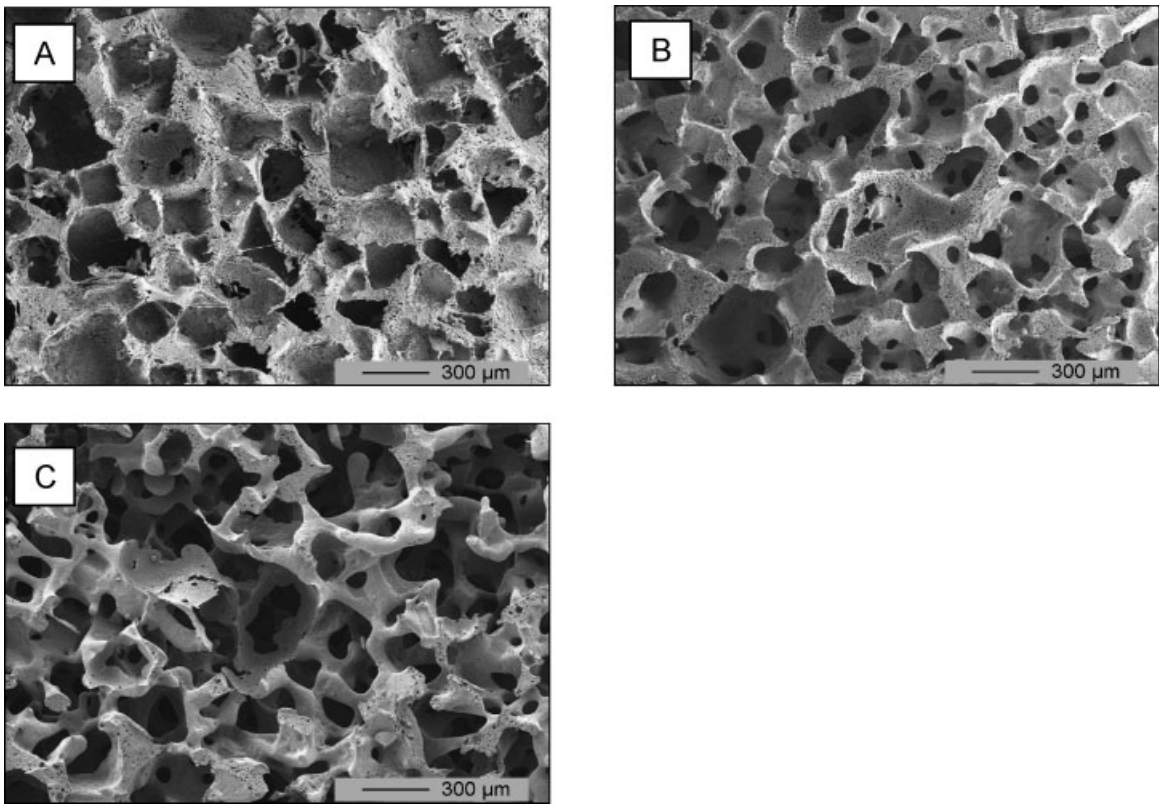

Figure 8. Foam structures obtained by cooling to −18°C a 35% PU1600 polymer solution in DMSO with variable amounts of water (A) 1.24%, (B) 2.45%, and (C) 10.7%.

Foam structure obtained with addition of water

The purpose of the addition of water to the DMSO solution of the polymer at 80°C is to decrease the solvent quality, and thus inducing a L–L phase separation process during cooling. The effect of the addition of different amounts of water on the foam structure is shown in Figure 8.

As already shown, with Estane foams the interconnectivity can be influenced by the use of water as a nonsolvent to induce liquid–liquid phase separation.[35] Also in this case more water leads to a better interconnectivity.

A speculative procedure for the formation of the interconnectivity is as follows: first the polymer-rich and poor phases are formed with the poor phase situated around the salt crystals. The polymer-poor phase is most likely to be nucleated on the surface of the NaCl crystals, which leads to a polymer-poor phase around the NaCl crystals.

Moreover, at that moment the system can be considered as three phases, namely the polymer-

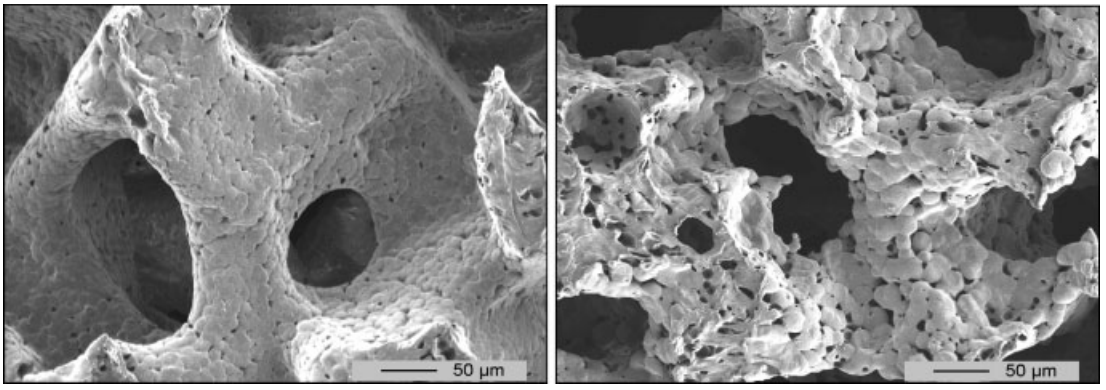

Figure 9. Cell wall morphology of foams prepared from a 35% PU1600 solution in DMSO with 7.5% water cooled to −18°C (left) and cooled to room temperature (right).

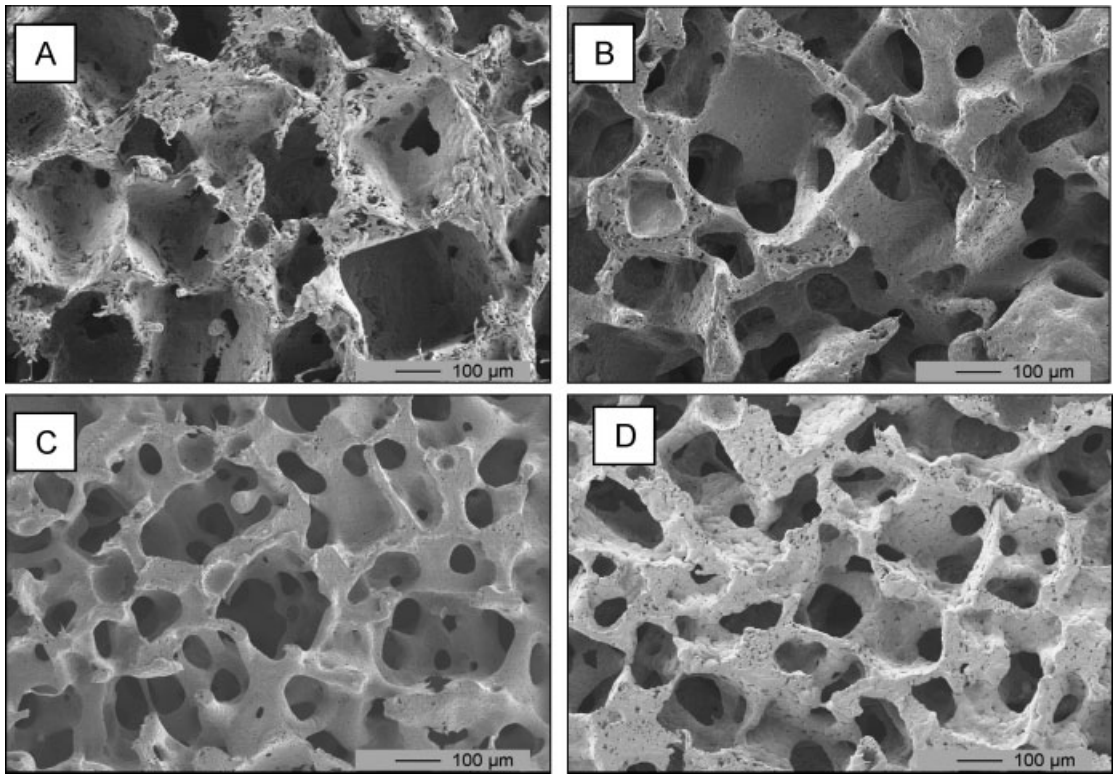

Figure 10. Foams made by cooling to −18°C based on different polymers (A) PU1000, (B) PU1600, (C) PU2200, and (D) PU2800.

rich phase, the polymer-lean phase, and the NaCl crystals. These three phases will try to minimize their interfacial energy.[37] It is known from literature that mixtures of three different homopolymers will do the same.[38] They will order in such a way that one phase/polymer will act as a compatibilizer, which intercalates between the two other more incompatible phases. Since the polymer is hydrophobic and the solvents are hydrophilic, in this case it is expected that it is energetically more favorable for the polymer-lean phase to wet the NaCl crystal surfaces than it is for the polymer-rich phase. When the proper composition is used the polymer-lean phase will wet the NaCl crystals and is able to form polymer-lean bridges between these crystals, which will lead to the interconnectivity.

Subsequently the NaCl, polymer-lean phase, and the solvent present in the polymer-rich phase are removed, which is followed by drying to yield the porous structure. It was noticed that the dimensions of the foams closely resembled the dimension of the polymer/salt/solvent mixture. Therefore it can be assumed that the pore dimensions correlate to the salt particle dimensions.

Moreover, cooling either to room temperature or to −18°C has a large influence on the cell wall structure (Fig. 9), which is analogous to the foams prepared without the presence of water (Fig. 7). Again no imprints from the DMSO crystals are present because washing was carried out at room temperature, above the DMSO melting point. Samples cooled to room temperature revealed a coarser spherulitic cell wall structure.

These structures were examined with a light microscope using crosspolarized filters and malteser crosses, which is an indication for the presence of spherulitic structures, as confirmed by SEM. The

TABLE II
Polymer, Water Concentration, and Porosity of the Foams Shown in Figure 10

	Polymer Concentration (wt %)	Water Concentration (wt %)	Porosity (%)	Hard Segment Content	Compression Modulus (kPa)
PU1000	36.0	6.5	80 ± 2	0.27	500 ± 30
PU1600	36.0	6.5	80 ± 2	0.19	380 ± 30
PU2200	32.4	6.5	83 ± 2	0.14	540 ± 30
PU2800	33.7	5.8	81 ± 2	0.12	1000 ± 30

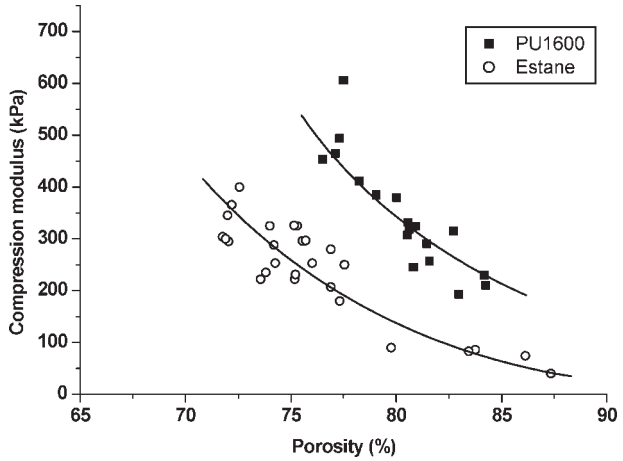

Figure 11. Influence of porosity on compression moduli of PU1600 foams in comparison with Estane foams[41] at 20% compression (particle size = 150–355 μm).

spheres are formed during gelation of hard segment, and the time and temperature of the gelation process determines the size of these spherulitic structures.

If, before washing, the polymer solutions are annealed at room temperature for different times a significant effect on the formation of these spherulitic foam wall structures was found. Annealing for 15 min gives small, sintered wall structures of roughly 15 μm (as determined from SEM pictures), while 90 min annealing yields spherical structures of roughly 27 μm in diameter, illustrating that time of gelation clearly influences the foam structure. A longer annealing time promotes the formation of bigger crystals.

Hard-segment content

The above-described method of foam production is not specific for PU1600. It is also possible to make foams of polyurethanes with a different polyol length as is shown in Figure 10, although they have similar porosities (Table II). The foams shown here were prepared in the same way and had overall porosities of 81% within experimental error. Because of the different polyester lengths the hard-segment contents of the polymers are different. This leads to a change in the overall compression modulus of the foams, what can be ascribed to differences in microphase separation and hard- and soft-segment crystallization. The pictures show that the difference in hard-segment content (and PCL length) leads to different structures. PU1000 shows a hairy structure on the cutting surface and only minor interconnectivity, PU2200 shows a smooth surface at this magnification, and good interconnectivity and PU2800 shows spherulitic-like structure with good interconnectivity. The term "good" means in this respect larger than the dimensions of the cells which have to move freely through the scaffold. The dimensions of average cells are 10–12 μm, so, clearly the scaffolds have the right interconnectivity.

The "bad" interconnectivity exhibited by the PU1000 might be ascribed to the early gelation (hard-segment crystallization) in solution before polymer liquid–liquid phase separation can take place. In that case, the primary foam structure is determined by the HS crystallization process, and the L–L phase separation phenomenon cannot change that situation anymore.

Compression

As mentioned earlier, the ratio between the amount of polymer, solvent, nonsolvent, and NaCl determines the total porosity of the resulting foam. Salt is a major factor in this process, since it forms the macropores which are needed for the ingrowth of tissue. The ideal situation is a very porous structure with pores of a suitable size[13] in combination with a high interconnectivity, without compromising the mechanical properties. However, an increase in total porosity decreases the compression modulus of the foam. As already mentioned in literature, the

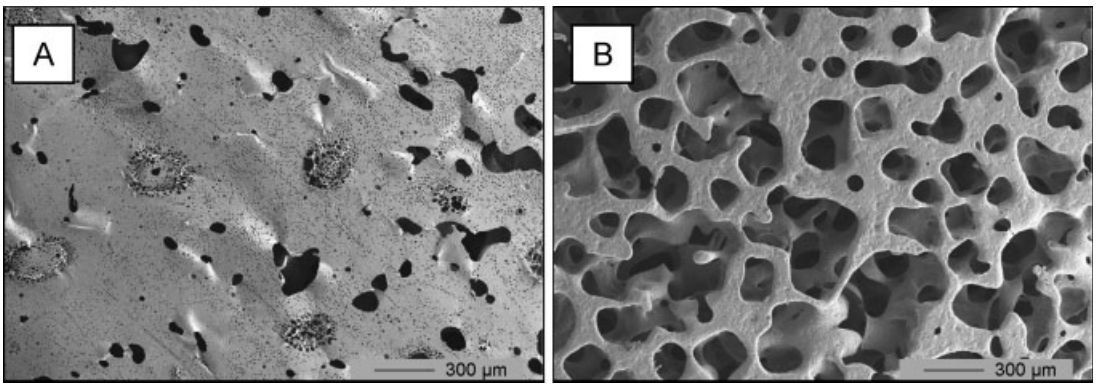

Figure 12. PU1600 foam with (left) and without (right) skin on the outer surface of the sample.

meniscus scaffold should have suitable mechanical properties to allow easy and reliable surgery and regeneration of new meniscus-like material.[39,40] Without a high resistance to tear, it would be impossible to fixate the scaffold in the knee joint, and the sutures probably would be torn out of the foam because of forces present in the knee.

The amount of NaCl and the amount of solvent are the main factors that determine the porosity of the scaffold.

Figure 11 shows the relation between porosity and compression modulus for the different foams made of PU1600 in comparison with Estane foams.[41] All the foams are based on a NaCl crystal size of 150–355 μm, whereas the water and salt content was varied in the preparation procedure to obtain different porosities. The compression modulus was determined from the compression curve at 20% compression. The Estane foams appeared to have much lower compression moduli at comparable porosities than the PU*x* series. This decrease can be related to the difference in Young's modulus between the polymers. A lower Young's modulus leads to a decrease in compression modulus, while the pore structure is only of minor influence here.[42]

If the hard-segment content of the polyurethane is changed, the fraction crystalline material changes too and consequently the mechanical properties, which is reflected in the compression modulus of foams made of different polymers (Table II).[27]

A decrease in hard-segment content causes a decrease in compression modulus, however, if the hard-segment content becomes less than about 0.2, a dramatic increase in compression modulus is observed. With high hard-segment contents there is only crystalline hard segment, while at the lower amounts of hard segment the soft-PCL segment is also able to crystallize, which again increases the total amount of crystalline material present in the foam. This causes the increase in compression modulus at lower hard-segment contents. We think it is not the amount of hard segment which determines the compression modulus, but the total amount of crystalline material present in the foam.

Skin removal

The preparation of scaffolds with a mould generally leads to the presence of a so-called skin. This skin is formed at the mould side by pushing the NaCl crystals away from the surface. This produces scaffolds with a more or less closed surface. One easily understands that this skin is a determinative barrier for the washing out of the scaffold and for cell ingrowth. The skin can be removed mechanically but this is more laborious and will make it more difficult to produce an accurate form. We found that it was possible to remove the skin during the foam production process. When the foams were dried after the washing with ethanol a skin was found, while if after the washing with ethanol the scaffolds are directly placed into a nonsolvent bath like ether or hexane the skin disappeared or opened completely (Fig. 12). Although the reason is not yet completely clear, it is tempting to speculate that it might be related to a delayed crystallization of the hard segments. During the preparation, the outer layer of the scaffold cools faster than to the inner parts of the scaffold. This in combination with a very thin skin layer might cause a too low crystallinity of the skin. Then, after swelling in ethanol combined with precipitation phenomena with ether, hard-segment crystallization takes place after all. This crystallization process causes the thin film to disappear. Although speculative, this explanation is also in agreement with the observation that if the ether treatment is carried out after drying the scaffold first at 37°C the skin did not disappear anymore. Moreover, after the skin removal, clear surface structures indicating spherulitic crystallization were found, whereas this is not the case before skin removal. Further research on this point is necessary. The removal of the skin during the foam making makes it possible to use moulds, and easily make predetermined shapes without the need of cutting the scaffold to remove the skin or shaping the foam to the scaffold form.

CONCLUSIONS

Polyurethanes described previously were used to prepare porous structures desired for scaffolds for tissue engineering.[27] The method described here is based on a combination of thermally induced phase separation and salt leaching of polymer dissolved in DMSO with water as nonsolvent. Upon cooling the polymer solution, liquid–liquid phase separation takes place, inducing the required interconnectivity of the macropores. The mechanical properties of the foams could be tuned by changing the overall porosity and the hard-segment content of the polymer. Foams with very high compression moduli (200 kPa–1 MPa), high porosities (76–84%) and excellent interconnectivity could be prepared.

When cooled to and annealed at room temperature it was found that spherulitic structures were formed, most likely because of the crystallization of the polymer. When DMSO crystallization was induced by cooling to −18°C spherulitic structure formation was suppressed and hardly visible.

With ATR-FTIR spectroscopy as a function of temperature it was clearly found that depending on the hard-segment content as well as the cooling procedure, soft segments and hard segments can crystallize.

The production of foams in moulds always leads to the formation of a skin at the outside of the foam. We were able to produce foams without a skin by applying an additional washing step.

Until now we have not found any limitation in foam size or shape. We made the foams with aid of several different (meniscus shaped) moulds, and the largest foam that was made was 4 cm × 4 cm × 4 cm.

This technique was found to be an excellent method to prepare highly interconnected and highly porous structures. We consider this as a highly versatile and promising method to obtain porous structures from elastomers.

The authors thank Mr. H. Nijland for the indispensable electron microscopic work and Ing. G. Alberda van Ekenstein for the assistance with DSC measurements.

References

1. Hou Q, Grijpma DW, Feijen J. Porous polymeric structures for tissue engineering prepared by a coagulation, compression moulding and salt leaching technique. Biomaterials 2003;24:1937–1947.
2. Hou Q, Grijpma DW, Feijen J. Preparation of porous poly(ε-caprolactone) structures. Macromol Rapid Commun 2002;23: 247–252.
3. Chen G, Ushida T, Tateishi T. Preparation of poly(L-lactic acid) and poly(DL-lactic-*co*-glycolic acid) foams by use of ice microparticulates. Biomaterials 2001;22:2563–2567.
4. Nam YS, Yoon JJ, Park TG. A novel fabrication method of macroporous biodegradable polymer scaffolds using gas foaming salt as a porogen additive. J Biomed Mater Res B 2000;53:1–7.
5. Spaans CJ, de Groot JH, Belgraver VW, Pennings AJ. A new biomedical polyurethane with a high modulus based on 1,4-butanediisocyanate and ε-caprolactone. J Mater Sci: Mater Med 1998;9:675–678.
6. Hutmacher DW, Schantz T, Zein I, Ng KW, Teoh SH, Tan KC. Mechanical properties and cell cultural response of polycaprolactone scaffolds designed and fabricated via fused deposition modeling. J Biomed Mater Res 2000;55:203–216.
7. Hua FJ, Kim GE, Lee JD, Son YK, Lee DS. Macroporous poly(L-lactide) scaffold 1. Preparation of a macroporous scaffold by liquid–liquid phase separation of a PLLA-dioxane-water system. J Biomed Mater Res B 2002;63:161–167.
8. Nam YS, Park TG. Biodegradable polymeric microcellular foams by modified thermally induced phase separation method. Biomaterials 1999;20:1783–1790.
9. van de Witte P, Esselbrugge H, Dijkstra PJ, van den Berg JWA, Feijen J. Phase transitions during membrane formation of polylactides. I. A morphological study of membranes obtained from the system polylactide-chloroform-methanol. J Membr Sci 1996;113:223–236.
10. Guan J, Fuijmoto K, Sacks M, Wagner W. Preparation and characterization of highly porous, biodegradable polyurethane scaffolds for soft tissue applications. Biomaterials 2006;26:3961–3971.
11. Stankus J, Guan J, Wagner W. Fabrication of biodegradable elastomeric scaffolds with sub-micron morphologies. J Biomed Mater Res A 2004;70:603–614.
12. Murphy WL, Dennis RG, Kileny JL, Mooney DJ. Salt fusion: An approach to improve pore interconnectivity within tissue engineering scaffolds. Tissue Eng 2002;8:43–52.
13. Elema H, De Groot JH, Nijenhuis AJ, Pennings AJ, Veth RPH, Klompmaker J, Jansen HWB. Use of biodegradable polymer implants in meniscus reconstruction. II. Biological evaluation of porous biodegradable implants in menisci. Colloid Polym Sci 1990;268:1082–1088.
14. Klompmaker J, Jansen HWB, Veth RP, Nielsen HKL, De Groot JH, Pennings AJ. Porous implants for knee joint meniscus reconstruction: A preliminary study on the role of pore sizes in ingrowth and differentiation of fibrocartilage. Clin Mater 1993;14:1–11.
15. Taylor DF, Smith FB. Porous methyl methacrylate as an implant material. J Biomed Mater Res Symp 1972;2:467–479.
16. Hulbert SF, Young FA, Mathews RS, Klawitter JJ, Talbert CD, Stelling FH. Potential of ceramic materials as premanently implantable skeletal prostheses. J Biomed Mater Res 1970; 4:433–456.
17. Taylor DF, Smith FB. Porous methyl methacrylate as an implant material. J Biomed Mater Res 1983;17:205–227.
18. Vacanti JP, Morse MA, Saltzmann WM, Domb AJ, Perez-Atayde A, Langer R. Selective cell transplantation using bioabsorbable artificial polymers as matrices. J Pediatr Surg 1988; 23:3–9.
19. Wake MC, Mikos AG, Sarakinos G, Vacanti JP, Langer R. Dynamics of fibrovascular tissue ingrowth in hydrogel foams. Cell Transplant 1995;4:275–279.
20. Klompmaker J, Jansen HWB, Veth RPH, de Groot JH, Pennings AJ, Kuijer R. Porous polymer implants for repair of meniscal lesions: A preliminary study in dogs. Biomaterials 1992;12:810–816.
21. Gorna K, Gogolewski S. Biodegradable porous polyurethane scaffolds for tissue repair and regeneration. J Biomed Mater Res A 2006;79:128–138.
22. De Groot JH, De Vrijer R, Pennings AJ, Klopmaker J, Veth RPH, Jansen HWB. Use of porous polyurethanes of meniscal reconstruction and meniscsal prosthesis. Biomaterials 1996;17: 163–173.
23. de Groot JH, Pennings AJ, Spaans CS, Wildeboer BS, de Vrijer R. New biomedical polyurethane ureas with high tear strengths. Polym Bull 1997;38:211–218.
24. van Tienen TG, Heijkants RGJC, Buma P, de Groot JH, Pennings AJ, Veth RPH. Tissue ingrowth and degradation of two biodegradable porous polymers with different porosities and poresizes. Biomaterials 2002;23:1731–1738.
25. van Tienen TG, Heijkants RGJC, Buma P, de Groot JH, Pennings AJ, Veth RPH. A porous polymer scaffold for meniscal lesion repair—A study in dogs. Biomaterials 2003;24:2541–2548.
26. Heijkants RGJC, van Calck RV, de Groot JH, Buma P, Pennings AJ, Veth RPH, Schouten AJ. Uncatalyzed synthesis, thermal and mechanical properties of polyurethanes based on poly(ε-caprolactone) and 1,4-butane diisocyanate with uniform hard segment. Biomaterials 2005;26:4219–4228.
27. Ramrattan NN, Heijkants RGJC, van Tienen TG, Schouten AJ, Veth RPH, Buma P. Assessment of tissue ingrowth rates in polyurethane scaffolds for tissue engineering. Tissue Eng 2005;11:1212–1223.
28. van Tienen TG, Heijkants RGJC, de Groot JH, Pennings AJ, Schouten AJ, Veth RPH, Buma P. Replacement of the knee meniscus by a porous polymer implant. Am J Sports Med 2006;34:64.
29. Heijkants RGJC, van Calck RV, van Tienen TG, Ramrattan N, Buma P, de Groot JH, Pennings AJ, Veth RPH, Schouten AJ. Design, synthesis and properties of a degradable polyurethane scaffold for meniscus regeneration. J Mater Sci: Mater Med 2004;15:423–427.

30. Heijkants RGJC, van Calck RV, de Groot JH, Pennings AJ, Schouten AJ. Phase transitions in segmented polyesterurethane–DMSO–water systems. J Polym Sci Part B: Polym Phys 2005;43:716–723.
31. Goris A. Test of the toxicity of dimethylsulfoxide (DMSO) on carrot tissue cultured in vitro. Ann Pharm Fr 1968;24:781–785.
32. Goris RJ. Treatment of reflex sympathetic dystrophy with hydroxyl radical scavengers. Unfallchirurgie 1985;88:330–332.
33. Rasmussen DH, MacKenzie AP. Phase diagram for the system water-dimethylsulphoxide. Nature 1968;220:1315–1317.
34. Arnauts J, De Cooman R, Vandeweerdt P, Koningsveld R, Berghmans H. Calorimetric analysis of liquid–liquid phase separation. Thermochim Acta 1994;238:1–16.
35. De Groot JH, Nijenhuis AJ, Bruin P, Pennings AJ, Veth RPH, Klompmaker J, Jansen HWB. Use of porous biodegradable polymer implants in meniscus reconstruction. I. Preparation of meniscus lesions. Colloid Polym Sci 1990;268: 1071–1081.
36. Crescenzi V, Manzini G, Calzolari G, Borri C. Thermodynamics of fusion of poly-β-propiolactone and poly-ε-caprolactone. Comparative analysis of the melting of aliphatic polylactone and polyester chains. Eur Polym J 1972;8:449–463.
37. van de Witte P, Dijkstra PJ, van den Berg JWA, Feijen J. Phase separation processes in polymer solutions in relation to membrane formation. J Membr Sci 1996;117:1–31.
38. Walheim S, Ramstein M, Steiner U. Morphologies in ternary polymer blends after spin coating. Langmuir 1999;15:4828–4836.
39. de Groot JH, Zijlstra FM, Kuipers HW, Pennings AJ, Klompmaker J, Veth RPH, Jansen HWB. Meniscal tissue regeneration in porous 50/50 copoly(L-lactide/ε-caprolactone) implants. Biomaterials 1997;18:613–622.
40. Klompmaker J. Porous polymers for the repair and replacement of knee joint meniscus and articular cartilage, Doctoral Thesis, University of Nijmegen, 1992, Chapter 6.
41. Heijkants RGJC, van Tienen TG, de Groot JH, Pennings AJ, Buma P, Veth RPH, Schouten AJ. Preparation of a polyurethane scaffold for tissue engineering made by a combination of salt leaching and freeze-drying of dioxane. J Mater Sci 2006;41:2423.
42. Gibson LJ, Ashby MF. Cellular Solids, Structure and Properties. Oxford: Pergamon Press; 1988. p 122–153.